Nonlinear absorption and optical limiting of platinum(Ⅱ) terpyridine complexes (*Invited*)

Sun Wenfang

(Department of Chemistry and Biochemistry, North Dakota State University, Fargo ND 58108-6050, United States)

Abstract: The reported work in 2003-2019 on the reverse saturable absorption (RSA) or two-photon absorption (TPA) and/or optical limiting (OPL) of platinum(II) terpyridine complexes was summarized in this minireview. Photophysical properties, including the ground-state absorption (GSA), excited-state absorption (ESA), excited-state lifetimes, and the quantum yields of triplet excited-state formation, RSA/OPL at 532 nm for ns laser pulses, TPA characteristics in the near-IR spectral regions, and the structure-property correlations were reviewed. This paper is composed of four sections. First, the current status of OPL materials and devices, the general requirements for reverse saturable absorbers and two-photon absorbing materials, and the different types and characteristics of square-planar platinum(II) complexes were briefly introduced. Then the photophysics and RSA/OPL of six series of Pt(Ⅱ) terpyridine-analogous complexes and the structure-property correlations were discussed. Following it the TPA of five series of Pt(Ⅱ) terpyridine complexes and the impacts of structural variations on the TPA cross sections (σ_2) were reviewed. Finally, brief conclusions were drawn based on the reported studies. A general trend discovered was that the charge transfer absorption band(s) and the ESA can be readily tuned by substituents on the acetylide or the terpyridine ligand. Introducing electron-donating substituent to the acetylide or terpyridine ligand or improving the coplanarity between the aromatic substituent and the terpyridine ligand red-shifted the ground-state charge-transfer absorption band(s) at the price of decreasing/quenching the triplet ESA, which consequently reduced the RSA/OPL at 532 nm. Extending the π-conjugation of the terpyridine ligand dramatically improved the σ_2 values of the Pt(Ⅱ) terpyridine complexes. Incorporation of electron-withdrawing π-conjugated aromatic substituent restrained the GSA to < 500 nm while keeping a long-lived triplet excited state with broadband ESA in the visible spectral regions and moderately strong TPA in the NIR regions. This approach could provide a solution for developing broadband OPL materials.

Key words: optical limiting; nonlinear absorption; platinum(Ⅱ) terpyridine complex; reverse saturable absorption; two-photon absorption

CLC number: O626 **Document code:** A **DOI:** 10.3788/IRLA20201078

联三吡啶铂(Ⅱ)配合物的非线性吸收和光限幅(特邀)

孙文芳

(北达克达州立大学 化学与生物化学系，美国 北达克达州法戈市 58108-6050)

摘　要：本文总结了 2003~2019 年报道的联三吡啶铂(Ⅱ)配合物的反饱和吸收或双光子吸收及光限

收稿日期:2020−09−18； 修订日期:2020−10−29

作者简介:Dr. Wenfang Sun (1968−), James A. Meier Senior Professor, Professor of Chemistry. Her research focuses on the development of organometallic/organic compounds for optical limiting, phototherapy, optical sensing, or bioimaging applications. Email: wenfang.sun@ndsu.edu

幅研究进展，并对这类配合物的光物理特性，包括基态吸收、激发态吸收、激发态寿命和三重态量子产率、在 532 nm 的反饱和吸收或光限幅，在近红外光区的双光子吸收，以及构效关系进行了评估。首先介绍了目前光限幅材料和器件的研究现状，对反饱和吸收和双光子吸收材料的基本要求，以及平面正方形铂(Ⅱ)配合物的种类和特性；其次讨论了六个系列联三吡啶类铂(Ⅱ)配合物的反饱和吸收或光限幅及构效关系；随后总结了五个系列联三吡啶铂(Ⅱ)配合物的双光子吸收及结构变化对双光子吸收截面的影响；最后对文献报道的工作进行了小结。根据文献报道的工作发现的一个趋势是：在联三吡啶配体或单齿炔配体上引入取代基可以调节基态和激发态的吸收，特别是在配体上引入给电子基团或增加联三吡啶和其上的芳香环取代基的共平面性会引起基态吸收红移但降低或淬灭激发态的吸收，这样会降低在 532 nm 的反饱和吸收或光限幅。但是扩展联三吡啶配体上的共轭体系则能大幅提高铂(Ⅱ)配合物的双光子吸收截面，尤其是在联三吡啶配体上引入吸电子的共轭芳香环取代基可以控制基态吸收在 500 nm 以下，同时保持了在可见光区的长寿命宽幅三重激发态吸收和在近红外光区的中等强度的双光子吸收，这对研制宽幅激光限幅材料有重要意义。

关键词： 光限幅；非线性吸收；联三吡啶铂(Ⅱ)配合物；反饱和吸收；双光子吸收

0 Introduction

In the past a few decades, lasers have been playing an indispensable role in many aspects of our lives, such as CD players, super market barcode readers and pocket laser pointer in our daily life; laser surgery in medicine; metal cutting and defect detection in industry; and laser weapons and ranging-finding, guidance and detection instruments in the military. The widespread use of lasers has increased the risk of accidental or intentional damage to human eyes and optical systems. There have been many reports in the news on the incidence of laser damage to optical systems and military personnel's eyes; and the potential to use commercial laser system as weapons becomes highly possible[1−4] . Such increased threat has triggered the development of optical limiting materials and devices for eye and sensor protections[5−16].

Generally, an ideal optical limiter should transmit 100% light at low incident laser intensity, but absorb, reflect, scatter or diffract most of the light when the laser intensity reaches the point that may cause damage to human eyes or optical sensors. The response time for the limiter should be faster than 1 ns. A broad spectral response that covers the visible to near-infrared (NIR) spectral range (400-900 nm) for protection of human eyes and night vision devices from the "frequency-agile" laser systems, and a broad temporal bandwidth effective for a variety of pulsed (< 1 ms) or CW (>1 ms) lasers are required. In addition, the material and device should have low toxicity and exhibit long-term stability. It should be able to operate at a variety of environments.

0.1 Current status for optical limiting materials and devices

Currently, the commercially available devices for eye and sensor protection include fixed-line filters that selectively eliminate 2-3 wavelengths (such as the laser protection goggles), neutral density filters, and mechanical or electro-optical shutters. However, the fixed-line filters have very low linear transmission (usually 10%-20%) and cause color distortion; neutral density filters are lack of contrast due to the overall low linear transmission; while the mechanical/electro-optical shutters have very slow response time and the optical systems are typically complicated. Most importantly, none of these devices can meet the requirement for broadband spectral and temporal responses. Therefore, new materials and device concepts are necessary for the development of new optical devices that can remove the threat of a laser beam but has a minimum impact on the optical system or on one's capability to commit mission. Meanwhile, the device must have broad spectral and temporal operating bandwidth.

To meet the aforementioned requirements for optical limiters, a variety of nonlinear optical mechanisms have

been investigated. Reverse saturable absorption (RSA), two-photon absorption (TPA), free-carrier absorption (FCA), nonlinear refraction (NLR), and nonlinear scattering have been found to be useful for passive reduction of optical transmission (the best approach to counter the frequency agile, short pulse threat)[5−16]. Because the performance of an optical limiter is predominantlydetermined by the properties of the material used in the device, seeking for optical limiting materials that exhibit one or multiple of the aforementioned nonlinear optical properties has been the major theme for the development of optical limiters. To date, the most widely investigated materials include semiconductors, carbon black suspensions, carbon nanotubes and graphene, organic compounds, organometallic complexes, liquid crystals, and organic/inorganic hybrids. Semiconductors typically exhibit low limiting threshold and good optical limiting performance; however, their damage thresholds are usually low. Carbon black suspensions (CBS) show broadband optical limiting extending to the NIR regions, but they must be used in liquid state and are subject to laser degradation. CBSs are not effective for ultrafast laser pulses (ps and fs lasers) either. Organic compounds or organometallic complexes typically possess fast time response and have high damage threshold, and the nonlinear optical properties can be readily tuned *via* structural modifications. Therefore, they would be better candidates to be developed into broadband optical limiting materials.

0.2 Reverse saturable absorption (RSA) and two-photon absorption (TPA)

RSA and TPA are two of the nonlinear optical phenomena in which the absorptivity of the absorber increases with the increased incident fluence or intensity. RSA occurs when a material has stronger excited-state absorption than that of the ground state at the interested wavelengths, which is a fluence-dependent process. TPA takes place when a material absorbs two photons of the same or different energies simultaneously to be populated to a virtue or real excited state of the material, thus the absorptivity depends on the square of the light intensity. TPA is an ultrafast and intensity-dependent process. Materials exhibiting strong RSA and/or TPA have potential applications in optical switching[17], optical limiting[18], laser mode locking[19], optical pulse shaping[20], spatial light modulation[20−21], laser beam compression[22], and TPA-induced photodynamic therapy[23], etc. Optical limiting devices based on RSA and/or TPA have the advantages of simple device design, broadband spectral and temporal responses.

For an ideal reverse saturable absorber, the molecule should have low but measurable ground-state absorption in the interested wavelength to populate the excited state; while the excited-state absorption cross section should be much larger than that of the ground state. The lifetime of the excited-state should be longer than the laser pulsewidth. For RSA of ns or longer laser pulses, a high triplet quantum yield is desired because the triplet excited-state absorption is the major contributor for absorbing longer pulsewidth laser beams. To meet these criteria, the conjugation length of the molecules should be carefully tuned because large π-conjugation would red-shift and increase the ground-state absorption cross sections in the visible spectral regions and thus reduce the ratios of the excited-state absorption cross section with respect to that of the ground state, which is a critical parameter for RSA. On the contrary, in order to increase the TPA crosssections of organic molecules, the molecules should possess extensive π-framework and/or strong intramolecularcharge transfer characters, which could decrease the transparency of the materials in the visible spectral regions. In addition, although the two-photon absorbing dyes can be almost 100% transparent in the NIR regions at low intensity, they usually only work for short-pulsewidth laser sources (ps or fs), not for longer pulsewidth lasers. Therefore, developing organic molecules that have light color (weak or no ground-state absorption in the spectral regions of 450-900 nm), but exhibit broad and strong excited-state absorption in the 450-900 nm regions and reasonable TPA in the NIR

regions is desired. In these molecules, RSA could occur in the green to red spectral regions; while two-photon induced excited-state absorption could induce optical limiting in the far-red to NIR regions. Combination of these nonlinear absorption phenomena could generate broadband optical limiting materials.

In organometallic complexes, the interactions between the metal center and the organic ligand generate multiple charge transfer excited states, which give rise to broad excited-state absorption. Selection of appropriate organic ligand could keep the major ground-state absorption bands to <450 nm. Meanwhile, heavy transition-metal complexes could exhibit high yield of triplet excited-state formation due to the heavy-atom enhanced intersystem crossing (ISC). Therefore, they are promising candidates for broadband optical limiting.

Among the variety of organometallic complexes that exhibits RSA, metallophthalocyanines possessing strong RSA in the visible spectral regions, such as lead-phthalocyanines (PbPc) or silicon naphthalocyanine (SiNc), are among the most promising ones. However, the strong linear absorption in the red to NIR regions prevents their application as broadband optical limiting materials in the NIR regions. To solve this problem, square-planar platinum(Ⅱ) complexes[24−25] may be good candidates.

0.3 Square-planar platinum(Ⅱ) complexes

Square-planar d^8 Pt(Ⅱ) complexes are interesting heavy transition-metal complexes with potential applications in DNA intercalation[26], protein probing[27], chemosensing[28], photovoltaic cells[29], light-emitting devices[30], catalysis[31], and optical limiting[32]. Figure 1 shows some representative structures for the most common types of square-planar Pt(Ⅱ) complexes, including Pt(Ⅱ)-bisphosphine bisacetylide complexes, Pt(Ⅱ) bipyridine bisacetylide complexes, and Pt(II) terdentate acetylide complexes. Among these complexes, Pt:ethynyl complexes are among the most well studied Pt(Ⅱ) complexes for nonlinear optics and optical limiting[32−38]. Unfortunately, these complexes suffered from instability upon laser irradiation, which limits their applications in practical optical limiting.

In contrast, Pt(Ⅱ) terdentate or diimine complex-exhibit excellent thermal and photochemical stabilities due to chelation of Pt(Ⅱ) ion by the terdentate or bidentate ligands. In addition, like the Pt:ethynyl complexes, the Pt(Ⅱ) terdentate or diimine complexes possess low ground-state absorption but strong excited-state absorption (ESA) in most of the visible to the NIR regions. The heavy-atom effect of the Pt(Ⅱ) ion facilitates the intersystem crossing and gives rise to a high triplet excited state population upon excitation, which would enhance the triplet excited-state absorption. Moreover, it is facile to conduct structural modifications on these complexes. The type of

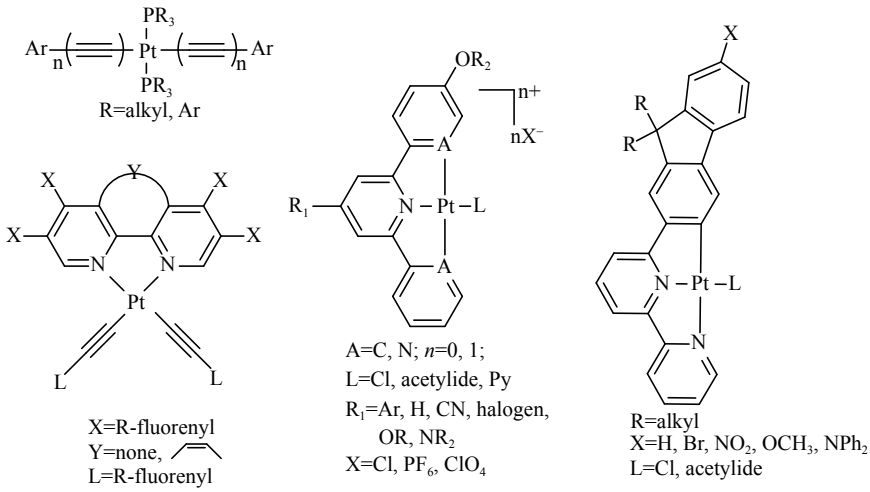

Fig.1 Representative structures for the most commonly studied square-planar Pt(II) complexes

terdentate ligand, the 4′-substituent on the terdentate ligand, and the monodentate co-ligand can be readily altered. The terdentate ligand could be assembled with other organic[39−41] or inorganic chromophores[42] and be used as building blocks for dendrimers[43−44]. It is also possible to assemble the mononuclear motif into *di*-, *tri*- and multinuclear complexes through a variety of bridging ligands[45−49]. Therefore, since our first report on the RSA-based optical limiting of Pt(Ⅱ) terdentate oligophenylacetylide complexes[50], our group and other groups have conducted an extensive study on the RSA/optical limiting and/or TPA of Pt(Ⅱ) terdentate complexes[51−77]. While the most common terdentate ligands include 2,2′:6',2″-terpyridine (N^N^N), 6-phenyl-2,2′-bipyridine (C^N^N), or 2,6-biphenylpyridine (C^N^C), this minireview will only focus on the RSA/optical limiting and/or TPA of Pt(Ⅱ) terpyridine complexes.

1 Reverse saturable absorption (RSA) and optical limiting of Pt(Ⅱ) terpyridine complexes at 532 nm

The first study on the RSA-based optical limiting of Pt(Ⅱ) terpyridine acetylide complexes (**1-3** in Fig.2) was reported by our group[50]. Those complexes contain oligophenylacetylide ligands with different degrees of conjugation and different substituents on the terpyridine ligand. The linear absorption spectra of the complexes (Fig.3(a)) exhibited strong absorption bands in the UV region (260-380 nm) that were assigned to $^1\pi,\pi^*$ transitions within the ligands; and broad bands in the 380-550 nm regions that were attributed to metal-to-ligand charge transfer (^{1}MLCT) transitions. Above 550 nm, the complexes were essentially transparent. Therefore, a broad optical window was formed at >500 nm, whereas the triplet excited state exhibited a broad absorption band (Fig.3(b)). Optical limiting of these complexes was demonstrated at 532 nm for 5 ns laser pulses. With a linear transmission of 90% in a 2 mm cuvette at 532 nm, the limiting thresholds (F_{th}) (defined as the incident fluence at which the transmission started to deviate from the linear transmission) for these complexes were found to be 20-30 mJ/cm^2; while the transmission decreased to 12-32% at the incident fluence of 3.6 J/cm^2 (Tab.1).

Both the linear absorption spectra and the transient difference absorption spectra are influenced by the degree of π-conjugation in the acetylide ligand. The complexes containing bis(phenylacetylide) ligand (**1** and **2**) exhibited a broader (380-830 nm) but slightly weaker excited-state absorption in the visible spectral region (500-780 nm) in contrast to **3** that possessed a monophenylacetylide ligand. Due to the weaker ground-state absorption at 532 nm for **3** but stronger excited-state absorption at this wavelength than those for **1** and **2**, complex **3** exhibited stronger optical limiting at 532 nm.

To quantitatively understand the excited-state cross section of **3**, Z-scan experiment was carried out for **3** at 532 nm using ns laser pulses, and the result was fitted by a five-energy-level model[57], which yielded a value of 5.5×10^{-17} cm^2 for the first triplet excited state absorption cross section (σ_{T1}), and is ~ 40 times as large as that of the ground state absorption ($\sigma_0=1.4\times10^{-18}$ cm^2). At high fluence (> 0.4 J/cm^2), the theoretical curve began to deviate from the experimental data, suggesting the presence of other nonlinear process. However, contribution from the nonlinear scattering was ruled out.

To evaluate the effects of arylacetylide ligand, our group studied a series of 4′-tolylterpyridine Pt(Ⅱ) complexes bearing different arylacetylide ligands (**4-10** in Fig.2)[52]. The photophysical properties and optical limiting performance of these complexes were systematically investigated. These complexes all exhibited intense ligand-localized $^1\pi,\pi^*$ absorption bands below 370 nm, and broad, moderately strong metal-to-ligand charge transfer (^{1}MLCT)/ligand-to-ligand charge transfer (^{1}LLCT) bands at 370-650 nm (Figs.4(a) and (b)). The separation of ^{1}MLCT band and ^{1}LLCT band became more salient when the electron-donating ability of the substituents at the phenyl ring increased and the ^{1}LLCT band red-shifted (see Fig.4(a) for **7** and **8**). However, only complexes **4-6** and **10** showed broad triplet excited-state absorption, with

4 and **5** possessing a narrower band at 350-430 nm and a broad band at 520-820 nm (Fig.4(c)). The transient absorption (TA) of **6** is much weaker, with only a broader band at 500-820 nm. In contrast, the TA of **10** is broader, with positive absorption bands appearing at 380-820 nm. The excited-state absorption of **7**, **8**, and **9** was too weak to be measured. Due to the lack of ground-state absorption of **6** at 532 nm and the non-detectable excited-state absorption of **7**, **8**, and **9**, optical limiting performance of only complexes **4**, **5** and **10** in CH_3CN at 532 nm was demonstrated. With a linear transmission of 70% in a 2 mm cuvette at 532 nm, the limiting threshold (defined as the incident fluence at which the transmission dropped to 90% of the initial linear transmission, i.e. at T/T_0 = 90%) varied from 0.049 J/cm^2 for **4**, 0.144 J/cm^2 for **5**, to 1.09 J/cm^2 for **10**; whereas the transmission dropped to 28% for **4**, 34% for **5**, and 44% for **10** (Fig.4(e) and Tab.2). The trend of the optical limiting strength **4**>**5**>**10** at 532 nm paralleled the trends of the triplet quantum yields (88±7% for **4**, 77±8% for **5**, and 60±5% for **10**), and of the ratios of the effective excited-state absorption cross section (σ_{eff}) vs. ground-state absorption cross

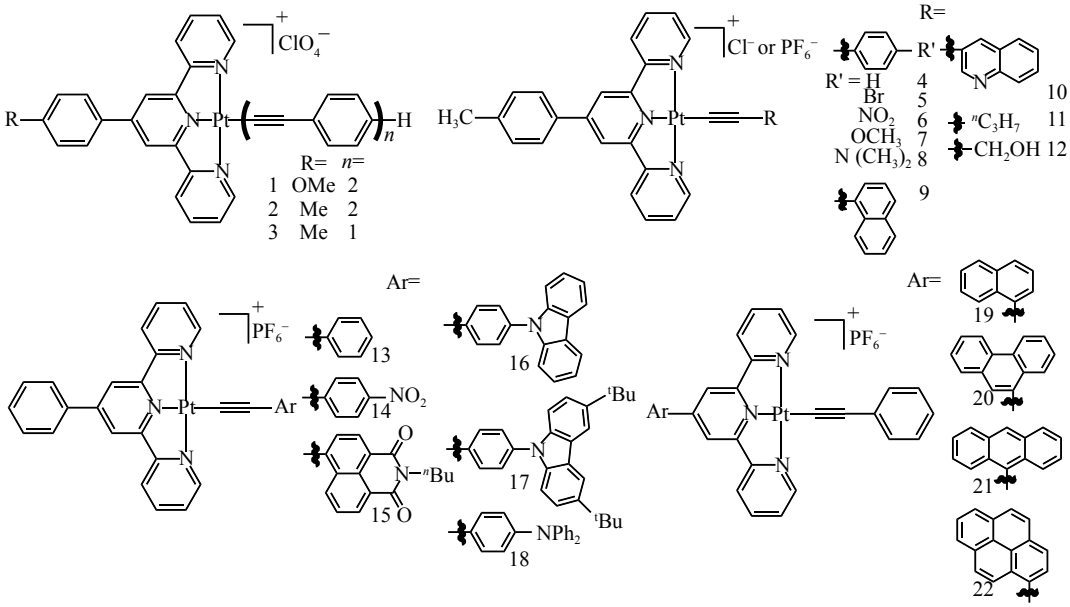

Fig.2 Structures of Pt(Ⅱ) terpyridine acetylide complexes **1-22** with different substituents on the acetylide ligand or on the terpyridine ligand

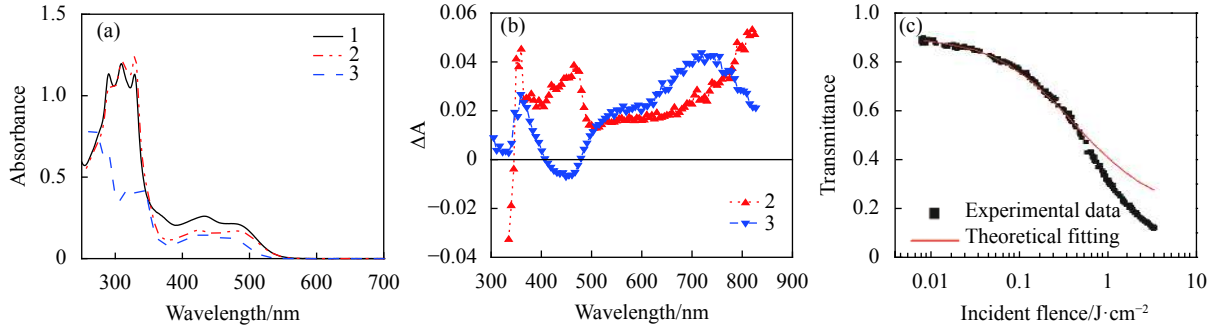

Fig.3 (a) Linear absorption spectra of complexes **1-3** (8.8×10^{-5} mol/L) in CH_2Cl_2/CH_3OH (8∶2) in a 2 mm cell, (b) triplet transient difference absorption (TA) spectra of **2** (2.39×10^{-5} mol/L) and **3** (2.09×10^{-5} mol/L) in a 1-cm cell. The TA spectrum of **1** was similar to that of **2**, thus was not shown in Fig.3(b), (c) Z-scan experimental data and fitting curve for **3** in CH_2Cl_2/CH_3OH (8∶2) with a concentration of 3×10^{-4} mol/L and a linear transmission of 95% at 532 nm in a 1 mm cell. Figures a and b are modified from Ref. [50] with permission, copyright © American Institute of Physics

Tab.1 Optical limiting parameters at 532 nm for ns laser pulses[a]

Complexes	F_{th}/J·cm^{-2}	$F_{throughput}$/J·cm^{-2}	T_{lim}(at 3.6 J·cm^{-2})
1	0.03	1.07	0.30
2	0.03	1.16	0.32
3	0.02	0.45	0.12

[a]Modified from Ref. [50] with permission. Copyright © American Institute of Physics

section (σ_g) at 532 nm for these complexes (Tab.2). It appeared that introducing electron-donating substituents (OCH_3 and $N(CH_3)_2$) on the phenylacetylide ligands diminished the triplet excited-state absorption and the optical limiting of the Pt(Ⅱ) terpyridine arylacetylide complexes.

In the work reported by Pritchett and Sun et al, the

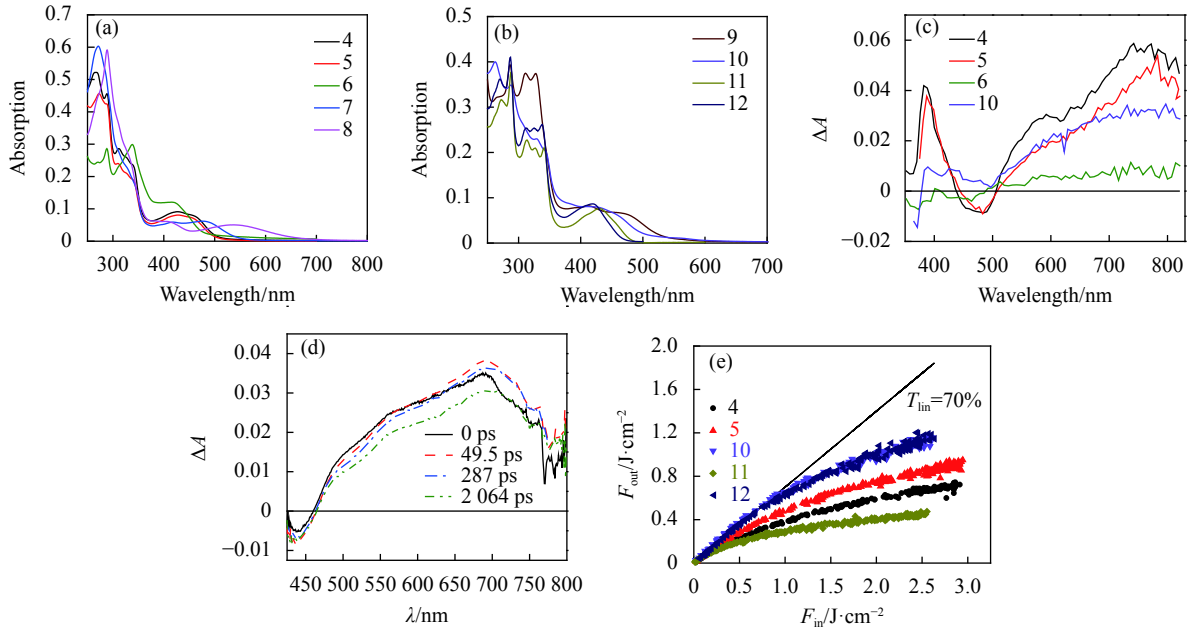

Fig.4 (a) and (b) Linear absorption spectra of complexes **4-12** (1×10^{-5} mol/L) in acetonitrile in a 1 cm cuvette, (c) ns TA spectra of **4, 5, 6** and **10** in acetonitrile in a 1 cm cell (A = 0.4 at 355 nm). See Ref. [51] for the ns TA spectra of **11** and **12** in acetonitrile, (d) time-resolved fs TA spectra of **11** in acetonitrile, (e) optical limiting curves of **4, 5, 10, 11** and **12** in acetonitrile in a 2 mm cell at 532 nm for 4.1 ns laser pulses. The linear transmission for all solutions was adjusted to 70% in the 2 mm cell. Figures are modified from Refs. [51] and [52] with permission, copyright © Chinese Optical Society and American Chemical Society, respectively

Tab.2 Photophysical parameters and optical limiting data for 4, 5, 10, 11, 12, and 19-22 in acetonitrile[51,53]

Complexes	τ_T/ns	σ_0 [c]/10^{-19}cm^2	F_{th} [d]/mJ·cm^{-2}	T_{lim} [e]	σ_{eff}/σ_0
4	766[a]	2.43	48	0.28[f], 0.25[g]	>3.57[f], >3.89[g]
5	659[a]	7.18	144	0.34[f]	>3.02[f]
10	672[a]	11.2	1 090	0.44[f]	>2.30[f]
11	62[a]	2.50[57]	62	0.19[f]	>4.66[f]
12	51[a]	2.40	900	0.45[f]	>2.24[f]
19	255[b]	18.1	250	0.27[g]	>3.67[g]
20	408[b]	4.30	370	0.27[g]	>3.67[g]
21	384[b]	17.6	490	0.32[g]	>3.19[g]
22	2 540[b]	13.4	52	0.18[g]	>4.81[g]

[a]Triplet excited-state lifetime deduced from the decay of the TA at 700 nm, from Ref.[51]. [b]Triplet excited-state lifetime deduced from the decay of the TA at 680 nm, from Ref.[53]. [c]Ground-state absorption cross section at 532 nm, from Refs. [51], [53] or [57]. [d]RSA threshold when the transmission dropped to 90% of the linear transmission. [e]Nonlinear transmittance at high incident fluence. [f]At incident fluence of 2.5 J/cm^2. [g]At incident fluence of 3.0 J/cm^2. This table is modified from Refs.[51] and [53] with permission. Copyrights © Chinese Optical Society and American Chemical Society, respectively

excited-state absorption of a 4-tolylterpyridyl Pt(Ⅱ) pentynyl complex **11** was investigated using Z-scan technique with ps and ns laser pulses at a variety of pulse energies at 532 nm[57]. This complex exhibited $^1\pi,\pi^*$ absorption bands below 360 nm, and ^{1}MLCT/^{1}LLCT bands at ca. 430 nm in CH_3CN, with a very low ground-state-absorption cross section of 2.5×10^{-19} cm^2 at 532 nm. On the other hand, both the singlet and triplet excited-state absorption of **11** was broad and strong in the regions of 470-800 nm (see Refs. [51] and [57] and Fig.4(d)). The singlet excited-state lifetime deduced from the decay of fs TA was (268±87) ps, while the triplet excited-state lifetime was 62 ns obtained from fitting the decay of ns TA signals. The triplet excited-state formation quantum yield was determined to be 0.16. By fitting the open-aperture picosecond and nanosecond Z-scan data using a five-level dynamic model, the singlet and triplet excited-stateabsorption cross sections were obtained to be 3.5×10^{-17} cm^2 and 4.5×10^{-17} cm^2, respectively. These values correponded to σ_S/σ_0 of 140 and σ_T/σ_0 of 180. The large ratio of σ_T/σ_0 made complex **11** a very strong optical limiting material for ns laser pulses at 532 nm. For an acetonitrile solution of **11** with a linear transmission of 70% in a 2 mm cuvette at 532 nm, **11** gave rise to the strongest optical limiting among complexes **4**, **5**, **10**, **11** and **12**, with a limiting threshold of 62 mJ/cm^2 (F_{th} at T/T_0 = 90%) and the transmission dropping to 19% at the incident fluence of 2.5 J/cm^2 for **11**[57].

Zhu and Liu 's group extended the study of different aryl substituents at the acetylide ligand on the RSA and optical limiting of the Pt(Ⅱ) 4′-phenyl-terpyridine complexes (**13-18** in Fig.2)[74]. Electron-withdrawing or donating aromatic substituents caused a blue- or red-shift of the low-energy ^{1}MLCT/^{1}LLCT absorption bands in these complexes, respectively. However, the electron-donating 4-carbozolylphenyl or 4-diphenylamino-phenyl motifs quenched the triplet excited-state absorption in complexes **16-18**; whereas the electron-withdrawing nitrophenyl or naphthylimidyl substituent reduced the triplet excited-state absorption coefficients and decreased the triplet excited-state formation quantum yields in **14** and **15**. Complexes **13-15** exhibited weak to moderate optical limiting at 532 nm, with a trend of **13**>**15**>**14**. For complex **13** that gave the strongest optical limiting, the limiting threshold at T/T_0 = 70% was found to be 0.30 J/cm^2, and the output fluence decreased to 0.97 J/cm^2 when the incident fluence reached ~2.5 J/cm^2.

To study the effects of substitution at the terpyridine ligands, our group reported a series of Pt(Ⅱ) 4′-aryl-terpyridine phenylacetylide complexes with 4′-naphthyl, 4′-phenanthryl, 4′-anthryl, and 4′-pyrenyl substituents (**19-22** in Fig.2)[53]. Similar to the other Pt(Ⅱ) terpyridine complexes **1-18**, these complexes possessed broad and moderately strong ^{1}MLCT/^{1}LLCT transitions at 390-525 nm. Different aryl substituents did not impact the energies of this band significantly (Fig.5(a)). However, both the TA spectral features and the triplet excited-state

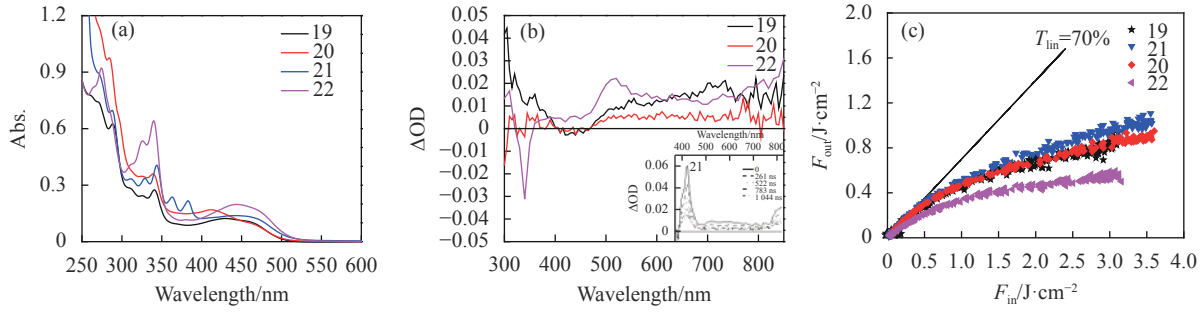

Fig.5 (a) Linear absorption spectra of **19-22** (2.0×10^{-5} mol/L) in acetonitrile in a 1 cm cuvette, (b) ns TA spectra of **19-22** in acetonitrile in a 1 cm cell (A = 0.4 at 355 nm), (c) optical limiting curves of **19-22** in acetonitrile in a 2 mm cell at 532 nm for 4.1 ns laser pulses. The linear transmission for all solutions was adjusted to 70% at 532 nm in the 2 mm cell. Figures are modified from Ref. [53] with permission, copyright © American Chemical Society

lifeitmes of these complexes were influenced by the aryl substituents drastically (Fig.5(b)). Complexes **21** and **22** possessed a broader TA at 380-830 nm than those for **19** and **20** (470-830 nm), with the maximum TA band apearing at approximately 520 nm for **22**. For **22**, its triplet excited state was found to have predominant 4′-pyrenylterpyridine ligand based intrali-gand charge transfer (^{3}ILCT)/$^3\pi,\pi^*$ characters, resulting in a much longer triplet excited-state lifeitme of 2.54 μs. All complexes exhibited optical limiting for 4.1 ns laser pulses at 532 nm in CH_3CN solutions with T_0 = 70% in a 2-mm cuvette at 532 nm, with **22** giving rise to the strongest optical limiting (Fig.5(c) and Tab.2). The limiting threshold of **22** was 52 mJ/cm^2 at T/T_0 = 90%, and the transmission decreased to 18% at the incident fluence of 3.0 J/cm^2. The strong optical limiting of **22** was ascribed to its much longer triplet excited-state lifetime and the stronger transient absorption at 532 nm.

For broadband optical limiting applications, it is important to broaden the ground-and excited-state absorption to longer wavelengths. Because the lowest-energy transition of an Pt(Ⅱ) terpyridine complex typically is the ^{1}MLCT state and the lowest unoccupied molecular orbital (LUMO) is localized at the terpyridine ligand, one of the approaches to red-shift the ground-state absorption is to lower the energy of the LUMO. One possible solution is to increase the coplanarity between the 4-aryl substituent and the central aza-aromatic ring at the terdentate ligand. Our group replaced the central pyridine ring with a 1, 3, 5-triazine ring on the terpyridine ligand for complexes **23**-**27** (Fig.6), which contained different monodentate ligands and different counter-anions[59]. Because of the electron-deficient nature of the triazine ring and the extension of π-conjugation between the terdentate ligand and the 4-(*p*-tolyl) substituent on the triazine ring associated with the increased coplanarity, these complexes exhibited bathochromic shifts in their UV-vis absorption spectra compared to their corresponding Pt(Ⅱ) terpyridine complexes (Fig.7(a)). It was found that the increased ligand field strength of the pentynyl or phenylacetylide ligand red-shifted the low-energy transitions in complexes **25**-**27** compared to those in **23** and **24**, which was the results of the red-shifted ^{1}MLCT transition and the occurrence of ^{1}LLCT transition. However, only complexes **25** and **26** exhibited broad and moderate triplet excited-state absorptions from 510 to 820 nm (Figs.7(b) and 7(c)). Nonlinear transmission experiment at 532 nm revealed that only **25**-**27** exhibited very weak optical limiting at 532 nm, with the optical limiting strength follows the trend of **25**>**26**>**27**. The stronger optical limiting of **25** was related to its lower ground-state absorption cross section (4.61×10^{-18} cm^2) but a higher triplet excited-state absorption cross section (1.20×10^{-17} cm^2) compared to those of **26** (5.25×10^{-18} cm^2 and 6.48×10^{-18} cm^2 for σ_0 and σ_T, respectively), which resulted in a higher ratio of σ_T/σ_0 for **25** (2.60) vs. that for **26** (1.23). For **27**, its much larger ground-state absorption cross section (1.28×10^{-17} cm^2) but non-detectable triplet excited-state absorption led to a much weaker optical limiting at 532 nm. Interestingly, although the counteranion showed a negligible effect on the energies of the ^{1}MLCT/^{1}LLCT states in **25** and **26**, it exerted a pronounced effect on the ^{3}MLCT state, reflected by the differences in emission efficiency (0.000 7 for **25** vs. 0.001 8 for **26**), the triplet excited-state extinction coefficient (ε_T (705 nm) = 3 400 M^{-1}·cm^{-1} for **25** vs. ε_T (705 nm) = 690 M^{-1}·cm^{-1}

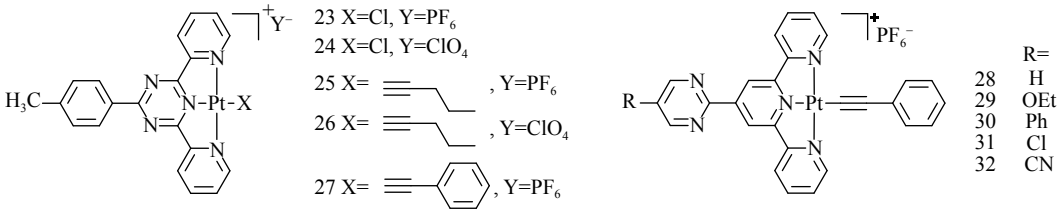

Fig.6 Structures of Pt(N^N^N) complexes **23**-**32**

for **26**), and the triplet quantum yield (0.21 for **25** and 0.83 for **26**), as well as on the optical limiting performance of these two complexes at 532 nm.

Another approach for improving the coplanarity within the N^N^N ligand is to replace the 4′-phenyl substituent on terpyridine ligand by a 4′-pyrimidyl substituent. Our group reported the photophysics and optical limiting of a series of 4′-(5‴-R-pyrimidyl)-2,2′;6′,2″-terpyridine platinum(Ⅱ) phenylacetylide complexes (**28-32** in Fig.6)[56]. These com-plexes possessed moderately intense ^{1}MLCT/^{1}LLCT transitions at ca. 400-500 nm in their UV-vis spectra, which were red-shifted in comparison to those of their corresponding 4′-toly-2,2′:6′,2″-terpyridyl platinum(Ⅱ) phenylacetylide complex, and influenced by the 5‴ substituents (Fig.8(a)). They also exhibited a linear correlation with the Hammett σ_p constant of the 5‴ substituent. These features demonstrated electron delocalization to the pyrimidyl substituent due to improved coplanarity between the pyrimidyl substituent and the terpyridine ligand. All complexes exhibited broad (500-820 nm) and strong singlet and triplet excited-state absorption with the absorption band being maximized at 720-785 nm (Fig.8(b)). Similar to the trend observed from the UV-vis absorption spectra, electron-donating substituent caused blue-shifted excited-state absorption (685 and 720 nm for singlet and triplet excited-state absorption, respectively) but a longer triplet lifetime (660 ns) in **30**; while electron-withdrawing substituent induced red-shifts (766 and 785 nm for singlet and triplet excited-state absorption, respectively, Tab.3) of the excited-state absorption and shortened the triplet lifetime (130 ns) in **32**. The singlet excited-state lifetimes were reported to be in the range of 37-139 ps for **28-32**[63]. Except for **30** (Φ_T = 0.19), the other four complexes

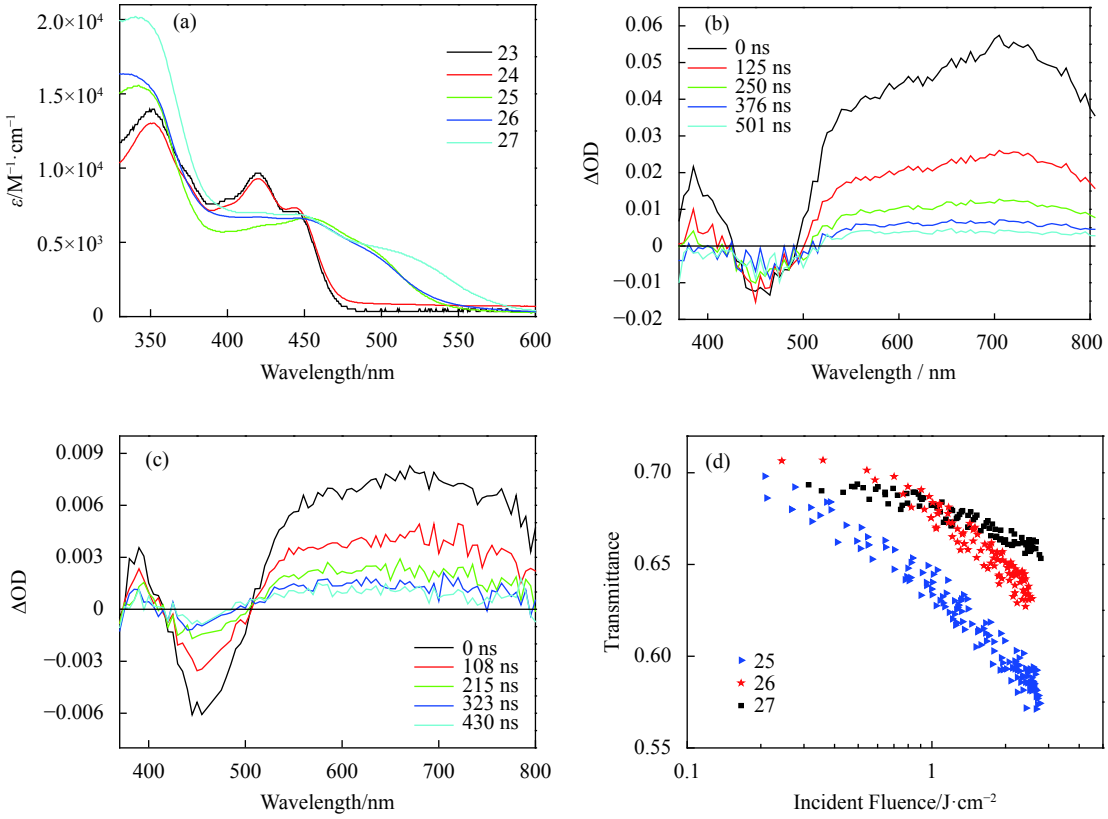

Fig.7 (a) Linear absorption spectra of **23-27** in CH_2Cl_2, (b) ns time-resolved TA spectra of **25** in CH_2Cl_2 in a 1 cm cell (6.2×10^{-5} mol/L (A_{355} = 0.888)), (c) ns time-resolved TA spectra of **26** in CH_2Cl_2 in a 1 cm cell (3.9×10^{-5} mol/L (A_{355} = 0.564)), (d) optical limiting curves of **25-27** in a 2 mm cell at 532 nm for 4.1 ns laser pulses. The linear transmission for all solutions was adjusted to 70% at 532 nm in the 2 mm cell. **25** and **26** were dissolved in CH_2Cl_2, and 27 was dissolved in DMF. Figures are modified from Ref. [5] with permission, copyright © American Chemical Society

exhibit high quantum yields of the triplet excited-state formation (0.53-0.66, see Tab.3). All complexes exhibited a moderate optical limiting at 532 nm for 4.1 ns laser pulses. The strength of the optical limiting followed the trend of **29**≈**28**≈**31**>**32**≈**30**.

Open-aperture Z-scan experiments using ns and ps lasers were carried out for **28-32** in CH_3CN solution at 532 nm, and the wavelength dispersion characteristics of **28** were investigated using ps laser pulses over the range of 500-600 nm[63]. Fitting the experimental Z-scan data using a five-level dynamic model gave rise to the singlet and triplet excited-state absorption cross sections (σ_s and σ_T, respectively) for **28-32** at 532 nm, which were in the range of $(18\pm1)\times10^{-18}$–$(50\pm5)\times10^{-18}$ cm^2 for σ_s and $(11\pm1)\times10^{-18}$–$(14\pm2)\times10^{-18}$ cm^2 for σ_T, and corresponded to σ_s/σ_0 ratios of 6.5-29.8 and σ_T/σ_0 ratios of 2.8-11.2 (Tab.4). Complexes **28**, **29** and **31** exhibited larger ratios of σ_s/σ_0 and $\sigma_T\Phi_T/\sigma_0$ than those of **30** and **32**. These trends

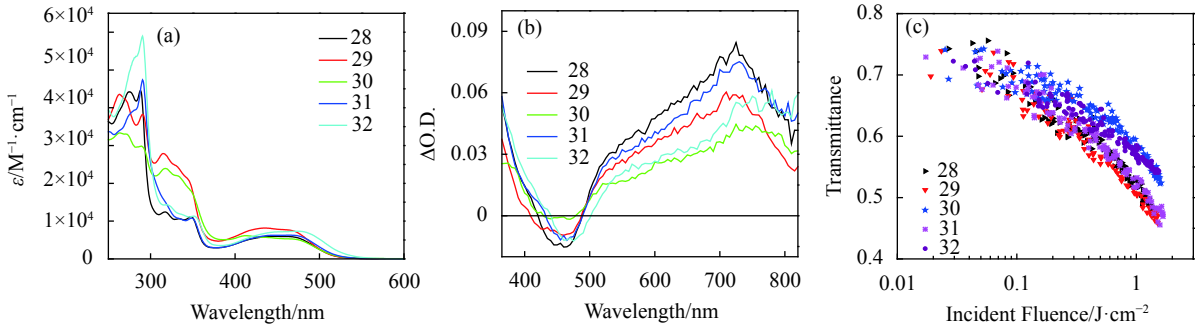

Fig.8 (a) Linear absorption spectra of **28-32** in acetonitrile, (b) ns TA spectra of **28-32** in acetonitrile in a 1 cm cell (λ_{ex} = 355 nm), (c) optical limiting curves of **28-32** in acetonitrile in a 2 mm cell at 532 nm for 4.1 ns laser pulses. The linear transmission for all solutions was adjusted to 75% at 532 nm in the 2 mm cell. Figures are modified from Ref.[56] with permission, copyright © American Chemical Society

Tab.3 Photophysical parameters of 28-32 in CH_3CN

	28	**29**	**30**	**31**	**32**
λ_{abs}/nm[a]	463	436	456	463	470
$\lambda_{S1\text{-}Sn}$/nm[b]	717	685	712	719	766
τ_s/ps[c]	37±23	56±17	139±128	42±8	46±16
$\lambda_{T1\text{-}Tn}$/nm[d]	725	720	755	730	785
τ_T/ns[e]	420	660	130	340	130
Φ_T[f]	0.65	0.53	0.19	0.64	0.66
τ_{isc}/ps[g]	57	106	732	66	70

[a] ^{1}MLCT/^{1}LLCT band maxima. [b]Femtosecond (fs) TA band maxima. [c]Singlet excited-state lifetimes. [d]Nanosecond (ns) TA band maxima. [e]Triplet excited-state lifetimes. [f]Quantum yields of the triplet excited-state formation. [g]Intersystem crossing (ISC) time. Data in rows 2 and 5-7 are from Ref. 56; data in rows 3, 4 and 8 are from Ref.[63], copyright © American Chemical Society and Old City Publishing, Inc., respectively

Tab.4 Ground-state and excited-state absorption cross sections of 28-32 in CH_3CN at 532 nm

	σ_0[a]/10^{-18} cm^2	σ_T[b]/10^{-18} cm^2	σ_T/σ_0	$\sigma_T\Phi_T/\sigma_0$	σ_s[c]/10^{-18} cm^2	σ_s/σ_0	σ_T[d]/10^{-17} cm^2	σ_T/σ_0
28	1.30	60.1	46.2	30.0	32±2	29.2	12±2	9.2
29	1.07	60.9	56.9	30.2	28±2	26.2	12±1	11.2
30	1.53	160	104.5	19.9	18±1	11.8	14±2	9.2
31	1.69	57.2	33.8	21.6	50±5	29.8	11±1	6.5
32	4.60	45.4	9.9	6.5	30±2	6.5	13±2	2.8

[a]Ground-state absorption cross-section. [b]Triplet excited-state absorption cross section deduced from the TA spectrum. [c]Singlet excited-state absorption cross sections obtained from fitting the Z-scan data. [d]Triplet excited-state absorption cross sections obtained from fitting the Z-scan data. Data in columns 2-5 are from Ref.[56]; while data in columns 6-9 are from Ref.[63], copyright © American Chemical Society and Old City Publishing, Inc., respectively

corresponded to the optical limiting trend for these complexes at 532 nm. In addition, the σ_s/σ_0 ratios of **28** increased drastically from 1.9 at 500 nm to 260 at 600 nm (Tab.5), implying that this complex could exhibit much stronger optical limiting at longer visible wavelengths.

Tab.5 Singlet excited-state absorption cross sections of 28 at different wavelengths[a]

λ/nm	$\sigma_0/10^{-18}$ cm^2	$\sigma_s/10^{-18}$ cm^2	σ_s/σ_0
500	9.18	17.5±0.5	1.9
532	1.30	38±2	29.2
550	0.709	27±1	38.1
570	0.302	15±2	49.7
600	0.096	25±2	260.4

[a]Obtained from the best-fit of ps Z-scan data, reported in Ref.[63]. Copyright © Old City Publishing, Inc

2 Two-photon absorption of Pt(Ⅱ) terpyridine complexes

Although many of the Pt(Ⅱ) terpyridine complexes exhibited broad and strong excited-state absorption extending from the visible to the NIR regions, the lack of ground-state absorption in the longer visible and NIR regions limited their applications as broadband optical limiting materials. To solve this problem, two approaches were employed. One of the approaches was to introduce stronger electron-donating groups to the acetylide ligand to increase the energy of the highest occupied molecular orbital (HOMO) or introducing electron-withdrawing substituents to the terpyridine ligand to lower the energy of the LUMO. Either of them would lower the ^{1}MLCT/^{1}LLCT transition energies and shift the low-energy absorption band to longer visible spectral regions. However, the red-shifted ground-state absorption spectra increased the ground-state absorption cross sections (σ_0), which significantly decreased the σ_{ex}/σ_0 ratios and reduced the optical limiting performances at 532 nm. Another possible approach is to incorporate two-photon absorbing unit to the complexes and utilize the two-photon induced excited-state absorption to broaden the nonlinear absorption windows to the NIR regions.

Our group reported three Pt(Ⅱ) chloride complexes **33**-**35** (Fig.9) bearing dipolar D-π-A terpyridine ligands, and investigated their photophysics and nonlinear absorption characteristics[67]. Electron-donating 7-diphenylamino-fluoren-2-yl motif was introduced to the terpyridine ligand *via* single, triple, or double bond in order to induce intraligand charge transfer in these complexes to increase their TPA cross sections (σ_2). The effect of the different linkers was evaluated as well. As shown in Fig.10, all three complexes exhibited red-shifted strong $^1\pi,\pi^*$/^{1}ILCT/^{1}MLCT absorption bands at 400-600 nm, and they gave broad excited-state absorption in the red to the NIR regions measured with the fs TA. Picosecond Z-scan measurements and the subsequent fitting with a five-level model gave the σ_s/σ_0 ratios of 2.0-131 for **33**, 2.6-78 for **34**, and 1.7-21 for **35** in the wavelength range of 575-670 nm (Tab.6). At wavelengths longer than 700 nm, the

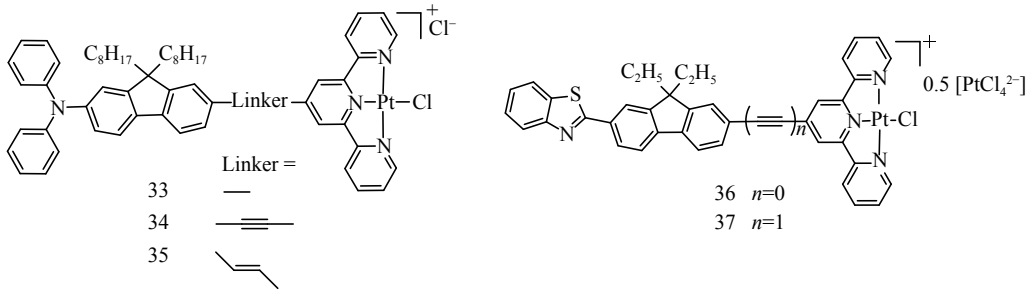

Fig.9 Structures of Pt(II) R-fluorenylterpyridine chloride complexes **33**-**37**

observed nonlinear absorption was attributed to TPA induced excited-state absorption. The σ_2 value(s) was 850 GM for **33** at 740 nm, and were 600-2000 GM at 740-825 nm for **34**. The TPA of **35** was too weak to be observed. Complex **34** with the ethynylene-linker showed much stronger TPA than complexes **33** and **35** with the single bond or vinylene-linker, likely due to the better conjugation provided by the ethynylene bridge between the terpyridine ligand and the diphenylaminofluorenyl motif.

Although the introduction of strong electron-donating diphenylamino substituent to the terpyridine ligand induced moderate TPA in the NIR regions in complexes **33-35**, the strong intramolecular charge transfer character shortened the triplet excited-state lifetimes so that the transient absorption in the ns time

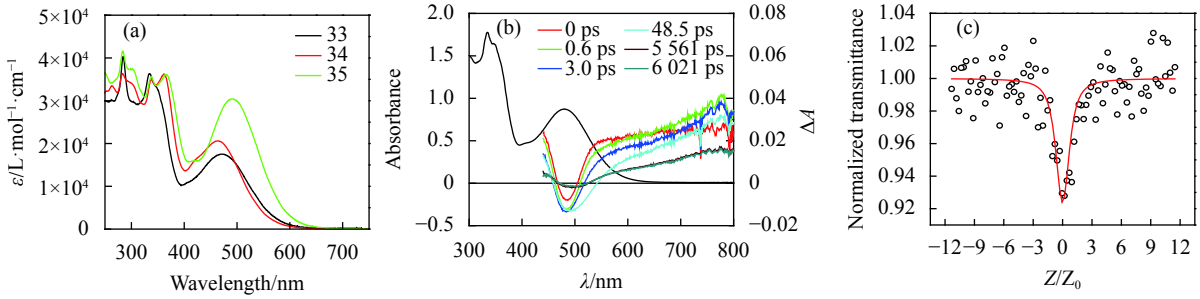

Fig.10 (a) UV-vis absorption spectra in CH_3CN for **33-35**, (b) time-resolved fs transient difference absorption spectra of **33** in CH_3CN, (c) open-aperture Z-scan experimental data and fitting curve for **34** in CH_3CN at 740 nm. The energy used for the experiment was 6.6 μJ, and the beam waist at the focal point was 31 μm. Figures are modified from Ref.[67] with permission, copyright © Wiley-VCH Verlag GmbH & Co. KGaA, Weinheim

Tab.6 Excited-state absorption and two-photon absorption cross sections for 33-35 at different wavelengths in CH_3CN

Complex	λ/nm	σ_0 /cm^{2a}	σ_S /10^{-18} cm^{2b}	σ_S/σ_0	σ_2 /GM
33	575	10.1	20±1	2.0	
	600	3.83	20±2	5.2	
	630	0.956	17±1	18	
	670	0.191	25±1	131	
	740		24.4[c]		850±50
34	550	14.7	38±2	2.6	
	575	6.31	24±2	3.8	
	600	2.49	24±2	9.6	
	630	0.765	26±2	34	
	680	0.153	12±1	78	
	740		7.7[c]		1 200±100
	760		11.1[c]		1 000±200
	800		7.7[c]		2 000±200
	825		11.6[c]		600±100
35	575	25.8	43±5[d]	1.7	
	600	10.9	36±2	3.3	
	630	3.63	20±2	5.5	
	670	0.765	16±1	21	

[a]Ground-state absorption cross sections. [b]Effective singlet excited-state absorption cross sections with the assumption of $\sigma_{S2} = \sigma_S$. [c]Estimated from the fs TA data at zero time delay. [d]$\sigma_{S2} = (12±7)\times10^{-18}$ cm^2. This table is modified from Ref.[67] with permission, copyright © Wiley-VCH Verlag GmbH & Co. KGaA, Weinheim

scale was unable to be observed. In addition, the strong ground-state absorption of these three complexes at 400-600 nm made them unsuitable for optical limiting in this spectral region. To retain the TPA in these Pt(Ⅱ) complexes while shifting the major absorption bands to below 450 nm, two Pt(Ⅱ) chloride complexes bearing 7-(benzothiazol-2′-yl)-9,9-diethylfluoren-2-yl substituted terpyridine ligands (**36** and **37** in Fig.9) were synthesized and studied by our group[72]. The 7-(benzothiazol-2′-yl)-9,9-diethylfluoren-2-yl substituent was attached to the 4'-position of the central pyridine ring of the terpyridine ligand *via* a single or triple bond linker. The band maxima of the low-energy absorption bands appeared at 428 nm and 433 nm for **36** and **37**, respectively (Fig.11(a)); while the triplet excited-state absorption was broad and strong in the spectral regions of 450-820 nm and maximized at 530 and 545 nm for **36** and **37**, respectively (Fig.11(b)). Meanwhile, the triplet excited states in these two complexes were long-lived (1.72-3.37 μs) and the triplet quantum yields were high (0.58-0.72, Tab.7). Therefore, both complexes exhibited pronounced optical limiting at 532 nm for ns laser pulses. With a linear transmission of

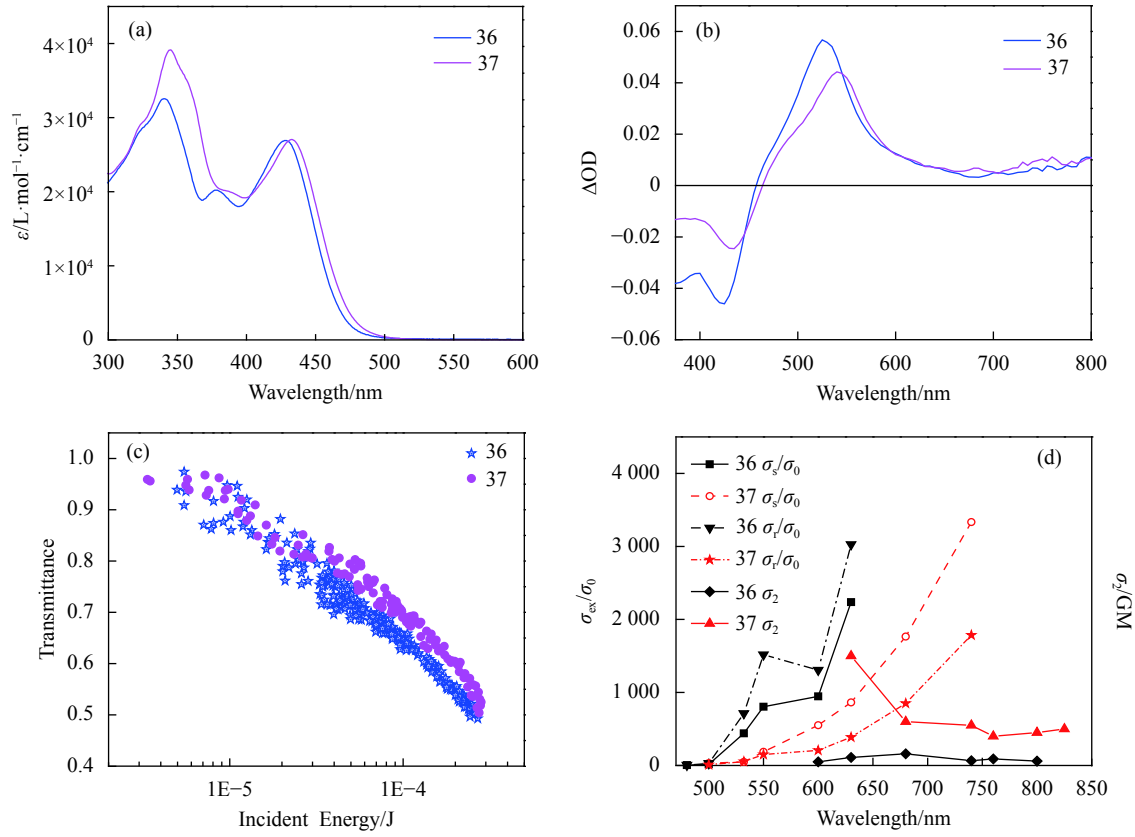

Fig.11 (a) UV-vis absorption spectra of **36** and **37** in DMSO, (b) nanosecond TA spectra of **36** and **37** in CH_3CN immediately after laser excitation. λ_{ex} = 355 nm. A_{355} = 0.4 in a 1 cm cuvette. (c) optical limiting curves of **36** and **37** in DMSO solution for 4.1 ns laser pulses at 532 nm. The linear transmission of the solution was adjusted to 95% in a 2 mm cuvette. The beam waist at the focal plane was 72 μm, (d) wavelength dispersion of the ratios of excited-state absorption cross section to that of the ground-state absorption (σ_{ex}/σ_0) and TPA cross section (σ_2) for **36** and **37** in DMSO solution. Figures are modified from Ref.[72] with permission, copyright © American Chemical Society

Tab.7 Photophysical parameters of 36 and 37[a]

	λ_{abs}/nm (ε/L·mol^{-1}·cm^{-1}) [b]	$\lambda_{S1\text{-}Sn}$/nm (τ_S/ps) [b]	$\lambda_{T1\text{-}Tn}$/nm (ε/L·mol^{-1}·cm^{-1}; τ_T/μs; Φ_T) [c]
36	340 (32550), 378 (20200), 428 (26900)	542 (49.4±18.3)	530 (48560; 3.37; 0.72)
37	345 (39140), 385 (sh. 20140), 433 (27040)	555 (58.7±25.4)	545 (46150; 1.72; 0.58)

[a]This table is modified from Ref.[72] with permission, copyright © American Chemical Society. [b]In DMSO. [c]In CH_3CN

95% in a 2 mm cuvette at 532 nm, the transmission decreased to <50% at an incident fluence of ~1.8 J/cm^2 (Fig.11(c)). Fitting of the Z-scan experimental data using the five-level model revealed that both complexes exhibited large ratios of the excited-state absorption cross sections vs. the ground-state absorption cross sections, with σ_s/σ_0 of 5.35-2 237 and σ_T/σ_0 of 5.35-3 026 for **36** at 480-630 nm, and σ_s/σ_0 of 31.8-3333 and σ_T/σ_0 of 10.6-1786 for **37** at 500-740 nm; and TPA cross sections of 50-200 GM for **36** at 600-900 nm and 400-3700 GM for **37** at 630-910 nm. It was noted that the σ_s/σ_0 and σ_T/σ_0 ratios of **36** are much larger than the corresponding ratios for **37** at most of the studied wavelengths due to the weaker ground-state absorption cross sections of **36** than those of **37** at each of the corresponding wavelength (Fig.11(d) and Tab.8). In contrast, the TPA cross sections of **37** are much larger than those of **36** at each of the corresponding wavelength due to the extended π-conjugation in **37** associated with the triple bond linker. The presence of RSA in the visible spectral regions and TPA initiated excited-state absorption in the NIR regions made these two complexes promising broadband optical limiting materials.

Very recently, Yam's group reported the TPA cross sections of two 1,3,5-triethynylbenzene-based alkynylplatinum(Ⅱ) terpyridine complexes (**38** and **39** in Fig.12) that were determined by two-photon induced fluorescence measurement[76]. The σ_2 values were reported to be 2 and 8 GM at 720 nm for **38** and **39**, respectively. The very small σ_2 values of this type of complexes could be attributed to the limited π-framework of the ligands in these complexes.

To improve the TPA of the alkynylplatinum(Ⅱ) terpyridine complexes, Yam's group reported a series of truxene-containing mononuclear or multinuclear alkynylplatinum(Ⅱ) terpyridine complexes **40**-**44** (Fig.12)[77]. The σ_2 values of **40** and **44** at 720 nm were measured by two-photon induced fluorescence and

Tab.8 Absorption cross sections of 36 and 37 at selected wavelengths determined by fitting of Z-scan data

λ/nm	$\sigma_0(\lambda)$[a]/10^{-18} cm^2		$\sigma_S(\lambda)$/10^{-18} cm^2		$\sigma_T(\lambda)$[c]/10^{-18} cm^2		σ_S/σ_0		σ_T/σ_0		$\sigma_2(\lambda)$/GM	
	36	**37**	**36**	**37**	**36**	**37**	**36**	**37**	**36**	**37**	**36**	**37**
480	5.23	–	28	–	28	–	5.35	–	5.35	–	–	–
500	1.41	1.32	22	42	40	14	15.6	31.8	28.4	10.6	–	–
532	0.095 5	0.390	42	19	68	21	440	48.7	712	53.8	–	–
550	0.043 5	0.187	35	35	66	28	805	187	1 517	150	–	–
600	0.022 2	0.072 6	21[b]	40	29	15	946	551	1 306	207	50	–
630	0.007 6	0.033 6	17[b]	29[b]	23	13	2 237	863	3 026	387	110	1 500
680	~0	0.015 3	19b	27[b]	23	13	−1 765		–	850	160	600
740	~0	0.008 4	22[b]	28[b]	31	15	−3 333		−1 786		65	550
760	~0	~0	22[b]	29[b]	36	16	–	–	–	–	90	400
800	~0	~0	22[b]	23[b]	53	20	–	–	–	–	60	450
825	~0	~0	–	43[b]	–	21	–	–	–	–	200[d]	500
850	~0	~0	–	–	–	–	–	–	–	–	280[d]	3 700[e]
875	~0	~0	–	–	–	–	–	–	–	–	180[d]	3 000[e]
900	~0	–	–	–	–	–	–	–	–	–	200[d]	–
910	~0	~0	–	–	–	–	–	–	–	–	–	1 700[e]

[a] Deduced from UV-Vis absorption spectrum. [b] Estimated from σ_S(532 nm) and the femtosecond transient difference absorption spectrum at zero time delay. These values are effective cross sections for the singlet excited states because the fs TA includes contributions from both S_1 and S_2 states. [c] σ_T(532 nm) was determined from the combined fitting of nanosecond and picosecond Z-scan data. For other wavelengths, $\sigma_T(\lambda)$ was estimated from σ_T(532 nm) and the femtosecond transient difference absorption spectrum at 5.9 ns time delay. [d] Effective TPA cross sections for excited-state-assisted TPA. [e] Effective TPA cross section for the *Z*-scan of lowest energy (11.5 μJ at 825 nm, 7.9 μJ at 850 nm, 8.3 μJ at 875 nm, and 10.0 μJ at 900 nm). This table is modified from Ref.[72] with permission, copyright © American Chemical Society

reported to be 37 and 108 GM, respectively. An obviously increased σ_2 value was achieved in **40** compared to that of **38**, and the increased σ_2 value of **44** with respect to that of **40** should be ascribed to the increased number of Pt(Ⅱ) terpyridine moieties.

Shi/Coe and co-workers reported the TPA of a trinuclear $RuPt_2$ and a heptanuclear $RuPt_6$ complexes by attaching $Pt^{Ⅱ}$ 2,2′:6′,2″-terpyridine (tpy) moieties to $Ru^{Ⅱ}$ 4,4′:2′,2″:4″,4‴-quaterpyridine (qpy) complexes (**45** and **46** in Fig.13)[73]. Z-scan measurement revealed higher TPA cross sections from these multinuclear complexes, with a maximal σ_2 value of 301 GM at 834 nm for $RuPt_2$ (**45**) and 523 GM at 850 nm for $RuPt_6$ (**46**). Attaching $Pt^{Ⅱ}$(tpy) moieties tripled or quadrupled the TPA cross sections of these multinuclear complexes when compared to the $Ru^{Ⅱ}$-based core. However, the electron-normalized maximal σ_2 values (σ_2/N_{eff}, where N_{eff} is the total number of π-bonding electrons in the complex (excluding the metal *d*-electrons)) were 0.043 and 0.016 GM for **45** and **46**, respectively, indicating no electronic interactions between the metal centers and thus no synergistic enhancement effects.

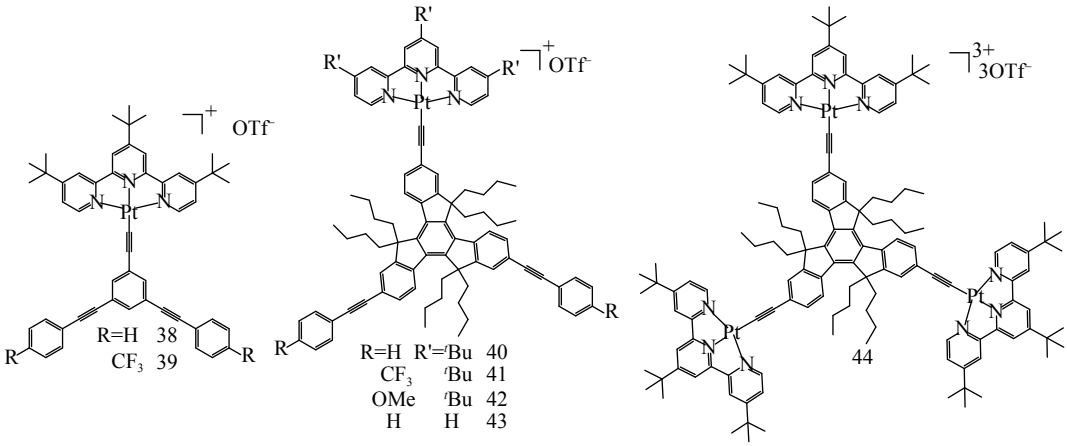

Fig.12 Structures of mononuclear or multinuclear alkynylplatinum(Ⅱ) terpyridine complexes **38**-**44**

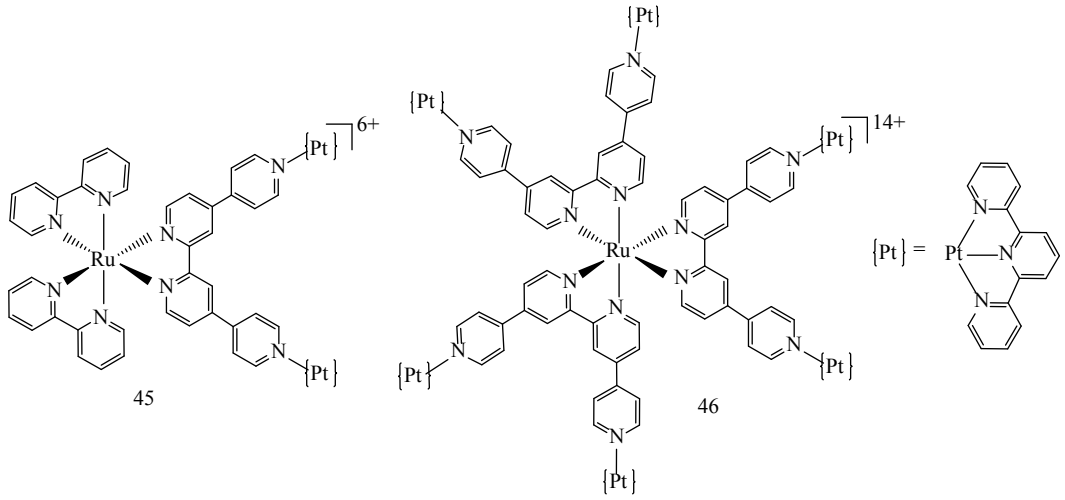

Fig.13 Structures of a trinuclear $RuPt_2$ and heptanuclear $RuPt_6$ complexes **45** and **46**

3 Conclusions

The reported work on the nonlinear absorption of Pt(Ⅱ) terpyridine complexes revealed that generally these complexes possessed weak ^{1}MLCT/^{1}LLCT ground-state absorption in the 400-600 nm spectral region, while the excited-state absorption of these complexes were broad and moderately strong at 500-800 nm. The ^{1}MLCT/

^{1}LLCT absorption band(s) and the excited-state absorption can be readily tuned by electron-donating or withdrawing substituents at the acetylide or the terpyridine ligand. Specially, introducing electron-donating substituent to the acetylide or terpyridine ligand, or improving the coplanarity between the aromatic substituent and the terdentate core ligand could red-shift the ^{1}MLCT/^{1}LLCT absorption band(s). Unfortunately, strong electron-donating substituents significantly reduced the triplet excited-state lifetime and consequently decreased/quenched the triplet excited-state absorption. Meanwhile, the red-shifted ^{1}MLCT/^{1}LLCT band(s) increased the ground-state absorption cross section at 532 nm and consequently reduced the RSA and optical limiting at 532 nm due to the reduced ratio of σ_{ex}/σ_0. The TPA cross sections (σ_2) of the Pt(Ⅱ) terpyridine complexes bearing small π-conjugated ligands were typically small. However, the σ_2 values could be dramatically improved by extending the π-conjugation on the terpyridine ligand. Particularly, incorporation of π-conjugated aromatic substituent without strong electron-donating ability could restrain the lowest-energy ground-state absorption band to <500 nm while keeping a long-lived triplet excited state with broadband excited-state absorption, and moderately strong TPA in the NIR regions. This approach could provide a solution for developing broadband optical limiting materials.

Acknowledgments

The author thanks the National Science Foundation (CHE 0449598) and the US Army Research Laboratory (W911NF 06-2-0032 and W911NF 10-2-0055) for financial-support.

References:

[1] Miller M J, Mott A G, Ketchel B P. General optical limiting requirements [C]//SPIE Conference on Nonlinear Optical Liquids for Power Limiting and Imaging, 1988, 3472: 24-29.

[2] Scott W B. Southwest pilot injured by laser [J]. Aviation Week and Space Technology, Nov. 20, 1995: 92.

[3] Gertz B. Russians fire laser at helicopter [N]. The Washington Times, 1997-05-14(A1).

[4] Pentagon is unable to link Russian laser to eye injury [N]. The Washington Post, 1997-06-27(A22).

[5] Bunning T J, Natarajan L V, Schmitt M G, et al. Optical limiting in solutions of diphenyl polyenes [J]. ***Applied Optics***, 1991, 30(30): 4341-4349.

[6] Soileau M J. Materials for Optical Switches, Isolators, and Limiters, Proc SPIE, vol. 1105 [C]. US: SPIE Press, 1989.

[7] Shirk J S, Pong R G S, Bartoli F J, et al. Optical limiter using a lead phthalocyanine [J]. ***Applied Physics Letters***, 1993, 63(14): 1880-1882.

[8] Soileau M J. Nonlinears Optical Materials for Switching and Limiting, Proc SPIE, vol. 2229 [C]. US: SPIE Press, 1994.

[9] Tutt L W, Kost A. Optical limiting performance of C_{60} and C_{70} solutions [J]. ***Nature***, 1992, 356: 225-226.

[10] Lawson C M. Nonlinear Optical Liquids and Power Limiters, Proc SPIE, vol. 3146 [C]. US: SPIE Press, 1997.

[11] Lawson C M. Nonlinear Optical Liquids for Power Limiting and Imaging, Proc SPIE, vol. 3472 [C]. US: SPIE Press, 1998.

[12] Lawson C M. Power-Limiting Materials and Devices, Proc SPIE, vol. 3798 [C]. US: SPIE Press, 1999.

[13] Eich M, Kuzyk M G, Lawson C M, et al. Linear, Nonlinear, and Power-Limiting Organics, Proc SPIE, vol. 4106 [C]. US: SPIE Press, 2000.

[14] Crane R, Lewis K, Van Stryland E, et al. Materials for optical limiting, MRS Proceedings, vol. 374 [C]. US: Materials Research Society Symposium, 1994.

[15] Sutherland R, Pachter R, Hood P, et al. Materials for optical limiting Ⅱ, MRS Proceedings, vol. 479 [C]. US: Materials Research Society Symposium, 1997.

[16] Nashimoto K, Pachter R, Wessels B W, et al. Thin films for optical waveguide devices and materials for optical limiting, MRS Proceedings, vol. 597 [C]. US: Materials Research Society Symposium, 2000.

[17] Li C, Zhang L, Wang R, et al. Dynamics of reverse saturable absorption and all-optical switching in C_{60} [J]. ***Journal of the Optical Society of America B***, 1994, 11(8): 1356-1360.

[18] Perry J W, Mansour K, Marder S R, et al. Enhanced reverse saturable absorption and optical limiting in heavy-atom-substituted phthalocyanines [J]. ***Optics Letters***, 1994, 19(9): 625-627.

[19] Penzkofer A. Passive Q-switching and mode-locking for the generation of nanosecond to femtosecond pulses [J]. ***Applied Physics B***, 1988, 46(1): 43-60.

[20] Reddy K P J. Applications of reverse saturable absorbers in laser science [J]. ***Current Issue***, 1991, 61(8): 520-525.

[21] Speiser S, Orenstein M. Spatial light modulation via optically induced absorption changes in molecules [J]. ***Applied Optics***, 1988, 27(14): 2944-2948.

[22] Yehuda B B, Harter D J, Raanan B. Optical pulse compressor composed of saturable and reverse saturable absorbers [J]. ***Chemical Physics Letter***, 1986, 126(3-4): 280-284.

[23] Shen Y, Shuhendler A J, Ye D, et al. Two-photon excitation nanoparticles for photodynamic therapy [J]. ***Chemical Society Reviews***, 2016, 45(24): 6725-6741.

[24] Gareth W J A. Photochemistry and Photophysics of Coordination Compounds: Platinum [M]//Vincenzo Balzani Sebastiano Campagna. Photochemistry and Photophysics of Coordination Compounds Ⅱ. Berlin: Springer, 2007: 205-268.

[25] Eryazici I, Moorefield C N, Newkome G R. Square-planar Pd(Ⅱ), Pt(Ⅱ), and Au(Ⅲ) terpyridine complexes: Their syntheses, physical properties, supramolecular constructs, and biomedical activities [J]. ***Chemical Reviews***, 2008, 108(6): 1834-1895.

[26] Lippard S J. Platinum complexes: probes of polynucleotide structure and antitumor drugs [J]. ***Accounts of Chemical Research***, 1978, 11(5): 211-217.

[27] Ratilla E M A, Brothers H M, Kostic N M. A transition-metal chromophore as a new, sensitive spectroscopic tag for proteins. Selective covalent labeling of histidine residues in cytochromesc with chloro(2,2':6'2"-terpyridine)platinum(Ⅱ) chloride [J]. ***Journal of the American Chemical Society***, 1987, 109(15): 4592-4599.

[28] Wong K M-C, Tang W-S, Lu X, et al. Functionalized platinum(Ⅱ) terpyridyl alkynyl complexes as colorimetric and luminescence pH sensors [J]. ***Inorganic Chemistry***, 2005, 44(5): 1492-1498.

[29] Wadas T J, Chakraborty S, Lachicotte R J, et al. Facile synthesis, structure, and luminescence properties of Pt(diimine)bis (arylacetylide) chromophore-donor dyads [J]. ***Inorganic Chemistry***, 2005, 44(8): 2628-2638.

[30] Lu W, Mi B, Chan M C W, et al. Light-emitting tridentate cyclometalated platinum(Ⅱ) complexes containing σ-alkynyl auxiliaries: Tuning of photo- and electrophosphorescence [J]. ***Journal of the American Chemical Society***, 2004, 126(15): 4958-4971.

[31] Fort Y, Comoy C. NHC—Nickel and —Platinum complexes in catalysis[J]. RSC Catalysis Series 6, 2011: 284-316.

[32] Staromlynska J, McKay T J, Bolger J A, et al. Evidence for broadband optical limiting in a Pt:ethynyl compound [J]. ***Journal of the Optical Society of America B***, 1998, 15(6): 1731-1736.

[33] McKay T J, Bolger J A, Staromlynska J, et al. Linear and nonlinear optical properties of platinum-ethynyl [J]. ***The Journal of Chemical Physics***, 1998, 108(13): 5537-5541.

[34] McKay T J, Staromlynska J, Davy J R, et al. Cross sections for excited-state absorption in a Pt:ethynyl complex [J]. ***Journal of the Optical Society of America B***, 2001, 18(3): 358-362.

[35] Price R S, Dubinina G, Wicks G, et al. Polymer monoliths containing two-photon absorbing phenylenevinylene platinum(Ⅱ) acetylide chromophores for optical power limiting [J]. ***ACS Applied Materials & Interfaces***, 2015, 7(20): 10795-10805.

[36] Yao C, Tian Z, Jin D, et al. Platinum(II) acetylide complexes with star-and V-shaped configurations possessing good trade-off between optical transparency and optical power limiting performance [J]. ***Journal of Materials Chemistry C***, 2017, 5(34): 11672-11682.

[37] Glimsdal E, Carlsson M, Kindahl T, et al. Luminescence, singlet oxygen production, and optical power limiting of some diacetylide platinum(Ⅱ) diphosphine complexes [J]. ***The Journal of Physical Chemistry A***, 2010, 114(10): 3431-3442.

[38] Cooper T M, Haley J E, Krein D M, et al. Two-photon spectroscopy of a series of platinum acetylides: Conformation-induced ground-state symmetry breaking [J]. ***The Journal of Physical Chemistry A***, 2017, 121(29): 5442-5449.

[39] Collin J-P, Harriman A, Heitz V, et al. Photoinduced electron- and energy-transfer processes occurring within porphyrin-metal-bisterpyridyl conjugates [J]. ***Journal of the American Chemical Society***, 1994, 116(13): 5679-5690.

[40] Harriman A, Odobel F, Sauvage J-P. Multistep electron transfer between porphyrin modules assembled around a ruthenium center [J]. ***Journal of the American Chemical Society***, 1995, 117(37): 9461-9472.

[41] Dixon I M, Collin J-P, Sauvage J-P, et al. Porphyrinic dyads and triads assembled around iridium(Ⅲ) bis-terpyridine: Photoinduced electron transfer processes [J]. ***Inorganic Chemistry***, 2001, 40(22): 5507-5517.

[42] Fang H, Du C, Qu S, et al. Self-assembly of the[60]fullerene-substituted oligopyridines on Au nanoparticles and the optical nonlinearities of the nanoparticles [J]. ***Chemical Physics Letters***, 2002, 364(3-4): 290-296.

[43] Newkome G R, Cardullo F, Constable E C, et al. Metallomicellanols: incorporation of ruthenium(Ⅱ)–2,2': 6',2″-

terpyridine triads into cascade polymers [J]. ***Journal of the Chemical Society, Chemical Communications***, 1993, 11: 925-927.

[44] Newkome G R, He E, Godínez L A, et al. Electroactive metallomacromolecules via tetrabis(2,2':6',2"-terpyridine) ruthenium(Ⅱ) complexes: Dendritic nanonetworks toward constitutional isomers and neutral species without external counterions [J]. ***Journal of the American Chemical Society***, 2000, 122(41): 9993-10006.

[45] Cheung T-C, Cheung K-K, Peng S-M, et al. Photoluminescent cyclometallated diplatinum(Ⅱ,Ⅱ) complexes: photophysical properties and crystal structures of $[PtL(PPh_3)]ClO_4$ and $[Pt_2L_2(\mu\text{-dppm})][ClO_4]_2$ (HL = 6-phenyl-2,2′-bipyridine, dppm = $Ph_2PCH_2PPh_2$) [J]. ***Journal of the Chemical Society, Dalton Transactions***, 1996, 8: 1645-1651.

[46] Lai S-W, Chan M C-W, Cheung T-C, et al. Probing d^8-d^8 interactions in luminescent mono- and binuclear cyclometalated platinum(Ⅱ) complexes of 6-phenyl-2,2'-bipyridines [J]. ***Inorganic Chemistry***, 1999, 38(18): 4046-4055.

[47] Lu W, Chan M C W, Cheung K-K, et al. π-π interactions in organometallic systems. crystal structures and spectroscopic properties of luminescent mono-, bi-, and trinuclear trans-cyclometalated platinum(Ⅱ) complexes derived from 2,6-diphenylpyridine [J]. ***Organometallics***, 2001, 20(12): 2477-2486.

[48] Lu W, Chan M C W, Zhu N, et al. Structural and spectroscopic studies on Pt···Pt and π-π interactions in luminescent multinuclear cyclometalated platinum(Ⅱ) homologues tethered by oligophosphine auxiliaries [J]. ***Journal of the American Chemical Society***, 2004, 126(24): 7639-7651.

[49] Wang Y, Yang Q, Wu L, et al. Synthesis and luminescent properties of an acetylide - bridged dinuclear platinum(Ⅱ) terpyridyl complex [J]. ***Chinese Journal of Chemistry***, 2004, 22(1): 114-116.

[50] Sun W, Wu Z, Yang Q, et al. Reverse saturable absorption of platinum ter/bipyridyl polyphenylacetylide complexes [J]. ***Applied Physics Letters***, 2003, 82(6): 850-852.

[51] Sun W , Guo F. Excited state absorption and optical limiting of platinum(Ⅱ) 4'-arylterpyridyl acetylide complexes [J]. ***Chinese Optics Letters***, 2005, 3(S): S34-S37.

[52] Guo F, Sun W, Liu Y, et al. Synthesis, photophysics, and optical limiting of platinum(Ⅱ) 4'-tolylterpyridyl arylacetylide complexes [J]. ***Inorganic Chemistry***, 2005, 44(11): 4055-4065.

[53] Guo F, Sun W. Photophysics and optical limiting of platinum(Ⅱ) 4'-arylterpyridyl phenylacetylide complexes [J]. ***The Journal of Physical Chemistry B***, 2006, 110(30): 15029-15036.

[54] Sun W, Zhu H, Barron P M. Binuclear cyclometalated platinum(Ⅱ) 4,6-Diphenyl-2,2'-bipyridine complexes: Interesting photoluminescent and optical limiting materialsng materials [J]. ***Chemistry of Materials***, 2006, 18(10): 2602-2610.

[55] Shao P, Sun W. Trinuclear platinum(Ⅱ) 4,6-diphenyl-2,2'-bipyridyl complex with bis(diphenylphosphinomethyl) phenylphosphine auxiliary ligand: synthesis, structural characterization, and photophysics [J]. ***Inorganic Chemistry***, 2007, 46(21): 8603-8612.

[56] Ji Z, Li Y, Sun W. 4′-(5‴-R-pyrimidyl)-2,2′:6′,2″-terpyridyl (R = H, OEt, Ph, Cl, CN) platinum(Ⅱ) phenylacetylide complexes: Synthesis and photophysics [J]. ***Inorganic Chemistry***, 2008, 47(17): 7599-7607.

[57] Pritchett T M, Sun W , Guo F, et al. Excited-state absorption in a terpyridyl platinum(Ⅱ) pentynyl complex [J]. ***Optics Letters***, 2008, 33(10): 1053-1055.

[58] Shao P, Li Y, Sun W. Cyclometalated platinum(Ⅱ) complex with strong and broadband nonlinear optical response [J]. ***The Journal of Physical Chemistry A***, 2008, 112(6): 1172-1179.

[59] Shao P, Li Y, Sun W. Platinum(Ⅱ) 2,4-Di(2′-pyridyl)-6-(p-tolyl)-1,3,5-triazine complexes: Synthesis and photophysics [J]. ***Organometallics***, 2008, 27(12): 2743-2749.

[60] Li Y, Pritchett T, Shao P, et al. Excited-state absorption of mono-, di- and tri-nuclear cyclometalated platinum 4,6-diphenyl-2,2′-bipyridyl complexes [J]. ***Journal of Organometallic Chemistry***, 2009, 694(23): 3688-3691.

[61] Ji Z, Azenkeng A, Hoffmann M, et al. Synthesis and photophysics of 4′-R-2,2′;6′,2″-terpyridyl (R = Cl, CN, $N(CH_3)_2$) platinum(Ⅱ) phenylacetylide complexestinum(Ⅱ) phenylacetylide complexes [J]. ***Dalton Trans***, 2009, 37: 7725-7733.

[62] Shao P, Li Y, Azenkeng A, et al. Influence of alkoxyl substituent on 4,6-diphenyl-2,2′-bipyridine ligand on photophysics of cyclometalated platinum(Ⅱ) complexes: Admixing intraligand charge transfer character in low-lying excited states [J]. ***Inorganic Chemistry***, 2008, 48(6): 2407-2419.

[63] Sun W, Li Y, Pritchett T, et al. Excited-state absorption of 4′-(5‴-R-pyrimidyl)-2,2′:6′,2″-terpyridyl platinum(Ⅱ) phenylacetylide complexes [J]. ***Nonlinear Optics, Quantum Optics: Concepts in Modern Optics***, 2010, 40(1): 163-174.

[64] Yi J, Zhang B, Shao P, et al. Synthesis and photophysics of platinum(Ⅱ) 6-Phenyl-4-(9,9-dihexylfluoren-2-yl)-2,2′-bipyridine complexes with phenothiazinyl acetylide ligand [J]. ***The Journal of Physical Chemistry A***, 2010, 114(26): 7055-7062.

[65] Liu R, Li Y, Li Y, et al. Photophysics and nonlinear absorption of cyclometalated 4,6-diphenyl-2,2′-bipyridyl platinum(Ⅱ) complexes with different acetylide ligands [J]. ***The Journal of Physical Chemistry A***, 2010, 114(48): 12639-12645.

[66] Shao P, Li Y, Yi J, et al. Cyclometalated platinum(Ⅱ) 6-phenyl-4-(9,9-dihexylfluoren-2-yl)-2,2′-bipyridine complexes: Synthesis, photophysics, and nonlinear absorption [J]. ***Inorganic Chemistry***, 2010, 49(10): 4507-4517.

[67] Ji Z, Li Y, Pritchett T M, et al. One-photon photophysics and two-photon absorption of 4-[9,9-Di(2-ethylhexyl)-7-diphenylaminofluoren-2-yl]-2,2′: 6′,2″-terpyridine and their platinum chloride complexes [J]. ***Chemistry-A European Journal***, 2011, 17(12): 2479-2491.

[68] Zhang B, Li Y, Liu R, et al. Synthesis, structural characterization, photophysics, and broadband nonlinear absorption of a platinum(Ⅱ) complex with the 6-(7-benzothiazol-2′-yl-9,9-diethyl-9 H-fluoren-2-yl)-2,2′-bipyridinyl Ligand [J]. ***Chemistry - A European Journal***, 2012, 18(25): 4593-4606.

[69] Li Z, Sun W. Synthesis, photophysics, and reverse saturable absorption of platinum complexes bearing extended π-conjugated C^N^N ligands [J]. ***Dalton Transactions***, 2013, 42(38): 14021-14029.

[70] Li Z, Badaeva E, Ugrinov A, et al. Platinum chloride complexes containing 6-[9,9-Di(2-ethylhexyl)-7-R-9H-fluoren-2-yl]-2,2′-bipyridine ligand (R = NO_2, CHO, benzothiazol-2-yl, n-Bu, carbazol-9-yl, NPh_2): Tunable photophysics and reverse saturable absorption [J]. ***Inorganic Chemistry***, 2013, 52(13): 7578-7592.

[71] Liu X, Sun W. Platinum(Ⅱ) complexes bearing 2-(9,9-dihexadecyl-7-R-fluoren-2-yl)-1,10-phenanthroline ligands: Synthesis, photophysics and reverse saturable absorption [J]. ***European Journal of Inorganic Chemistry***, 2013, 2013(27): 4732-4742.

[72] Zhang B, Li Y, Liu R, et al. Extending the bandwidth of reverse saturable absorption in platinum complexes using two-photon-initiated excited-state absorption [J]. ***ACS Applied Materials & Interfaces***, 2013, 5(3): 565-572.

[73] Shi P, Coe B J, Sánchez S, et al. Uniting ruthenium(Ⅱ) and platinum(Ⅱ) polypyridine centers in heteropolymetallic complexes giving strong two-photon absorption [J]. ***Inorganic Chemistry***, 2015, 54(23): 11450-11456.

[74] Zhao T, Liu R, Shi H, et al. Synthesis, tunable photophysics and nonlinear absorption of terpyridyl Pt(Ⅱ) complexes bearing different acetylide ligands [J]. ***Dyes and Pigments***, 2016, 126: 165-172.

[75] Fang B, Zhu Y, Hu L, et al. Series of C^N^C cyclometalated Pt(Ⅱ) complexes: Synthesis, crystal structures, and nonlinear optical properties in the near-infrared region [J]. ***Inorganic Chemistry***, 2018, 57(22): 14134-14143.

[76] Po C, Tao C-H, Li K-F, et al. Design, synthesis, luminescence and non-linear optical properties of 1,3,5-triethynylbenzene-based alkynylplatinum(Ⅱ) terpyridine complexes [J]. ***Journal of Organometallic Chemistry***, 2019, 881: 13-18.

[77] Po C, Tao C-H, Li K-F, et al. Design, luminescence and nonlinear optical properties of truxene-containing alkynylplatinum(Ⅱ) terpyridine complexes [J]. ***Inorganica Chimica Acta***, 2019, 488: 214-218.